Acta Oceanol. Sin., 2018, Vol. 37, No. 9, P. 107–115
DOI: 10.1007/s13131-018-1270-9
http://www.hyxb.org.cn
E-mail: hyxbe@263.net

Recent satellite-derived sea ice volume flux through the Fram Strait: 2011–2015

BI Haibo[1, 2, 3, 4], WANG Yunhe[1, 2, 3, 4*], ZHANG Wenfeng[5], ZHANG Zehua[1, 2, 3, 4], LIANG Yu[1, 2, 3, 4], ZHANG Yi[1, 2, 3, 4], HU Wenmin[6], FU Min[7], HUANG Haijun[1, 2, 3, 4*]

[1] Key Laboratory of Marine Geology and Environment, Institute of Oceanology, Chinese Academy of Sciences, Qingdao 266071, China

[2] Laboratory for Marine Geology, Pilot National Laboratory for Marine Science and Technology (Qingdao), Qingdao 266200, China

[3] Center for Ocean Mega-Science, Chinese Academy of Sciences, Qingdao 266071, China

[4] University of Chinese Academy of Sciences, Beijing 100049, China

[5] Shidao Meteorological Observatory of Shandong Province, Weihai 264309, China

[6] Wenchang Campus of China University of Mining and Technology, Xuzhou 221008, China

[7] National Marine Environmental Forecasting Center, State Oceanic Administration, Beijing 100081, China

Received 23 October 2018; accepted 28 December 2018

Abstract

The Fram Strait (FS) is the primary region of sea ice export from the Arctic Ocean and thus plays an important role in regulating the amount of sea ice and fresh water entering the North Atlantic seas. A 5 a (2011–2015) sea ice thickness record retrieved from CryoSat-2 observations is used to derive a sea ice volume flux via the FS. Over this period, a mean winter accumulative volume flux (WAVF) based on sea ice drift data derived from passive-microwave measurements, which are provided by the National Snow and Ice Data Center (NSIDC) and the Institut Francais de Recherche pour d'Exploitation de la Mer (IFREMER), amounts to 1 029 km^3 (NSIDC) and 1 463 km^3 (IFREMER), respectively. For this period, a mean monthly volume flux (area flux) difference between the estimates derived from the NSIDC and IFREMER drift data is –62 km^3 per month (–18×10^6 km^2 per month). Analysis reveals that this negative bias is mainly attributable to faster IFREMER drift speeds in comparison with slower NSIDC drift data. NSIDC-based sea ice volume flux estimates are compared with the results from the University of Bremen (UB), and the two products agree relatively well with a mean monthly bias of (5.7±45.9) km^3 per month for the period from January 2011 to August 2013. IFREMER-based volume flux is also in good agreement with previous results of the 1990s. Compared with P1 (1990/1991–1993/1994) and P2 (2003/2004–2007/2008), the WAVF estimates indicate a decline of more than 600 km^3 in P3 (2011/2012–2014/2015). Over the three periods, the variability and the decline in the sea ice volume flux are mainly attributable to sea ice motion changes, and second to sea ice thickness changes, and the least to sea ice concentration variations.

Key words: sea ice volume flux, Fram Strait, CryoSat-2

Citation: Bi Haibo, Wang Yunhe, Zhang Wenfeng, Zhang Zehua, Liang Yu, Zhang Yi, Hu Wenmin, Fu Min, Huang Haijun. 2018. Recent satellite-derived sea ice volume flux through the Fram Strait: 2011–2015. Acta Oceanologica Sinica, 37(9): 107–115, doi: 10.1007/s13131-018-1270-9

1 Introduction

Climatic and environmental changes in the arctic have a significant impact on the mass balance of sea ice (Comiso, 2012; Steele and Ermold, 2015; Stroeve and Notz, 2015; Lei et al., 2016b). The most important dynamic mechanism associated with variations in a sea ice mass balance is ice export via the Fram Strait (FS), through which roughly 10% of the Arctic sea ice cover is transported southwards into the Greenland Sea and the downstream North Atlantic region (Zhang et al., 2000; Kwok et al., 2004; Lei et al., 2016a; Smedsrud et al., 2017). The associated export of fresh water could result in a great salt anomaly and perhaps broad geophysical consequences through the modulation of the global deep-water conveying belt system (Koenigk et al., 2006; Serreze et al., 2007).

Owing to the limited knowledge of the cross-strait sea ice thickness distribution, previous studies have mostly focused on the retrieval of a sea ice area flux from a satellite-derived ice drift speed and concentration fields (Vinje, 2001; Kwok et al., 2004, 2005; Kwok, 2009; Krumpen et al., 2013; Bi et al., 2016b; Smedsrud et al., 2017). However, the sea ice volume flux, which incor-

Foundation item: The National Natural Science Foundation of China under contract No. 41406215; the Foundation of Laboratory for Marine Geology, Institute of Oceanology, Chinese Academy of Sciences; the Foundation of Qingdao National Laboratory for Marine Science and Technology; the Postdoctoral Science Foundation of China under contract No. 2014M561971; the Open Fund for the Key Laboratory of Marine Geology and Environment, Institute of Oceanology, Chinese Academy of Sciences under contract No. MGE2013KG07; the NSFC-Shandong Joint Fund for Marine Science Research Centers under contract No. U1606401.
*Corresponding author, E-mail: yhw1118@yeah.net; hjhuang@qdio.ac.cn

porates the contribution of the sea ice thickness, is a more relevant parameter pertaining to sea ice mass balance (Vinje et al., 1998; Kwok et al., 2004; Spreen et al., 2009; Bi et al., 2016a). Despite of paucity of the sea ice thickness observations in the FS, which are sparse in spatial and temporal details, several attempts have been directed to estimate the sea ice volume flux through the FS. For example, the sea ice thickness fields provided by several moored upward looking sonar (ULS) were extrapolated to obtain the cross-strait profile of the sea ice thickness, allowing the retrieval of the FS sea ice volume flux for the period of the 1990s (Vinje et al., 1998; Kwok et al., 2004). In a report by Spreen et al. (2009), the sea ice thickness retrieved from ICESat observations was utilized to estimate the FS sea ice volume flux for the period of 2003–2008. Also, attempts to obtain the FS sea ice volume flux during the summer months were carried out through applying the airborne electromagnetic (AEM) ice thickness measurements for the period of 2001–2012 (Krumpen et al., 2016). Moreover, to construct a consistent time series (1990–2013) of the FS sea ice volume export, Spreen (personal communication) compiled a cross-strait sea ice thickness profile based on three to four ULS measurements deployed in the FS region around 79°N (Spreen et al., 2016).

Unlike the sea ice drift and concentration fields, the sea ice thickness is not a routinely observed parameter from field and/or satellite measurements. Therefore, the above-mentioned sea ice volume flux estimates are greatly restricted in their spatial and temporal resolutions. For instance, the ICESat was expected to be used to establish the monthly averaged thickness filed over the arctic sea ice cover. However, the satellite operates only for two or three one-month campaigns within a year (Kwok et al., 2009). Thus, the obtained monthly sea ice volume flux estimates (October–April) over 2003–2008 were retrieved based on the interpolated ICESat sea ice thickness fields (Spreen et al., 2009). The moored ULS instruments observe the overpassing floating sea ice every several seconds with a low uncertainty level, but the limited number of available moorings is not able to capture the variability of the cross-strait sea ice thickness (Hansen et al., 2013, 2014, 2015). On the other hand, radar altimeters onboard the European Space Agency (ESA) satellites, such as European remote sensing satellites (ERS) (Laxon et al., 2003) and Envisat (Giles et al., 2008), can provide the sea ice thickness for winter months (October–May), despite a coarse spatial resolution (about 10 km). Recently, a new ESA satellite, CryoSat-2 (CS2), carries a synthetic aperture radar (SAR)/Interferometric Radar altimeter (SIRAL) and observes the sea ice thickness at a fine surface resolution, namely, 0.31 km by 1.67 km (Laxon et al., 2013). Moreover, this satellite is unique for its northernmost scope of observations (up to 88°N), leaving a much reduced data gap around the North Pole compared with its predecessors, such as ICESat (86°N) and ESA satellites (84°N). This study is mainly motivated by the possibility to monitor the cross-strait sea ice thickness distribution from CS2 (Laxon et al., 2013; Kwok and Cunningham, 2015), such that the time series of the sea ice volume flux through the FS can be further extended to the period from 2011 to 2015.

This paper is organized as follows. Section 2 describes the data and the methodology used to compute the sea ice area and volume flux. Section 3 presents the area and volume flux estimates based on different data sources of satellite-derived ice drifts (IFREMER and NSIDC). Meanwhile, comparisons between pervious sea ice volume flux estimates from different sea ice drift data sources are outlined. Section 4 analyzes the changes of the volume flux over different periods and discuss the association with the sea ice drift, sea ice thickness and the sea ice concentration. Concluding remarks are given in Section 5.

2 Data and methodology

2.1 *Sea ice volume flux estimation*

The sea ice volume flux (F_v) across a flux gate corresponds to the integral of the product of three parameters, including the gate-perpendicular component of the ice motion (u), the ice concentration (c), and the thickness (T) along the gate. Accordingly, it can be written as

$$F_v(j) = G\sum_{i=1}^{N} u_i c_i T_i, \tag{1}$$

where j denotes a winter month between October and April; N is the number of grid cells along the gate; and G is the width of a grid cell. Here, the width of a grid cell is set to 25 km (NSIDC) or 62.5 km (IFREMER) depending on the input sea ice drift data set. The flux gate (bold black line as shown in Fig. 1) selected for this study spans a length of approximately 400 km (roughly along 81°N). Regarding the terminology and sign convention, outflow (i.e., positive fluxes) refers to the export of sea ice from the Arctic Ocean, while inflow (i.e., negative fluxes) refers to the northward advection of sea ice towards the Arctic Ocean.

Assuming that the uncertainty of the volume flux estimates for the grid samples are additive, unbiased, uncorrelated, and normally distributed, the uncertainty with respect to the monthly sea ice volume flux across the FS can be computed as

$$\sigma_{Fv} = G\left\{\sum_{i=1}^{N}\left[(\sigma_{u_i}c_iT_i)^2 + (\sigma_{c_i}u_iT_i)^2 + (\sigma_{T_i}u_ic_i)^2\right]\right\}^{1/2}, \tag{2}$$

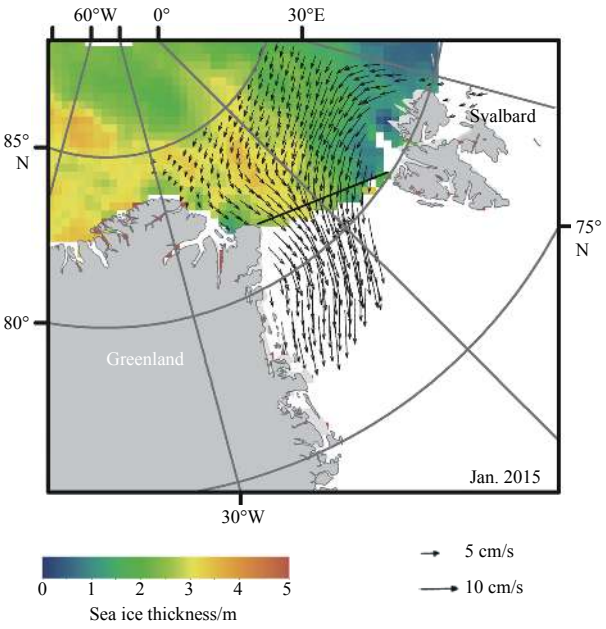

Fig. 1. Location of the flux gate (black bold line) used to determine FS sea ice outflow. Sample NSIDC drift vectors (arrows, January 2015) around the FS area are presented. CS2-derived sea ice thickness of the corresponding month is denoted by the blue-to-red color.

where σ_u, σ_c and σ_T are the uncertainties at the ith grid of the monthly mean ice motion, concentration and thickness, respectively. For the uncertainty of the sea ice concentration (σ_c), an uncertainty value of 12% is used for winter months (Meier, 2005). For the uncertainty of sea ice motion (σ_u) (Kwok, 2009), we use

$$\sigma_u = \frac{\sigma_\mathrm{d}}{\sqrt{n}}, \tag{3}$$

where n is the number of valid sea-ice drift estimates available for a grid cell in 1 month; σ_d is the uncertainty of a single ice drift. For the uncertainty of the single ice drift (σ_d), we use the upper limit of the uncertainty determined through comparisons with buoy drifts, which corresponds to 3.45 km/d (or 4 cm/s) for the IFREMER product (Girard-Ardhuin and Ezraty, 2012) and 1.73 km/d (or 2 cm/s) for NSIDC sea ice drift data (Sumata et al., 2014). For the uncertainty of sea ice thickness (σ_T), we use a value of 0.62 m, which represents the standard deviation of the difference between CS2-derived thickness and NASAs Operation IceBridge (OIB) airborne measurements as we provided in Fig. 2.

Winter accumulative volume flux (WAVF) can be calculated as

$$F_{WAVF} = \sum_{j=\mathrm{Oct.}}^{\mathrm{Apr.}} F_v(j). \tag{4}$$

The uncertainty of the F_{WCV} is then obtained with the following equation:

$$\sigma_{WAVF} = \sqrt{\sum_{j=\mathrm{Oct.}}^{\mathrm{Apr.}} \sigma^2_{F_v(j)}}. \tag{5}$$

2.2 *Satellite-derived data*

2.2.1 *Sea ice drift*

Polar Pathfinder Sea Ice Motion Vectors (Version 3) provided by the NSIDC have a grid spacing of 25 km and span the period of 1978–2015. Multiple sources of sea ice motion vectors are combined to establish the NSIDC sea ice drift data, including satellite-based data from the SMMR, SSM/I, AMSR-E and AVHRR, as well as buoy and wind observations. The monthly mean drift data (http://nsidc.org/data/NSIDC-0116) have uncertainties ranging from 1 to 2 cm/s as a function of sea ice concentration and drift rate (Sumata et al., 2014).

For comparison, another sea ice drift dataset provided by the IFREMER is also utilized to compute sea ice outflow. It represents a merged product of the ice drift retrieved from the SSM/I and ASCAT observations available for the winter months (October–April) over the period of 2011–2015 (hereafter, refer this

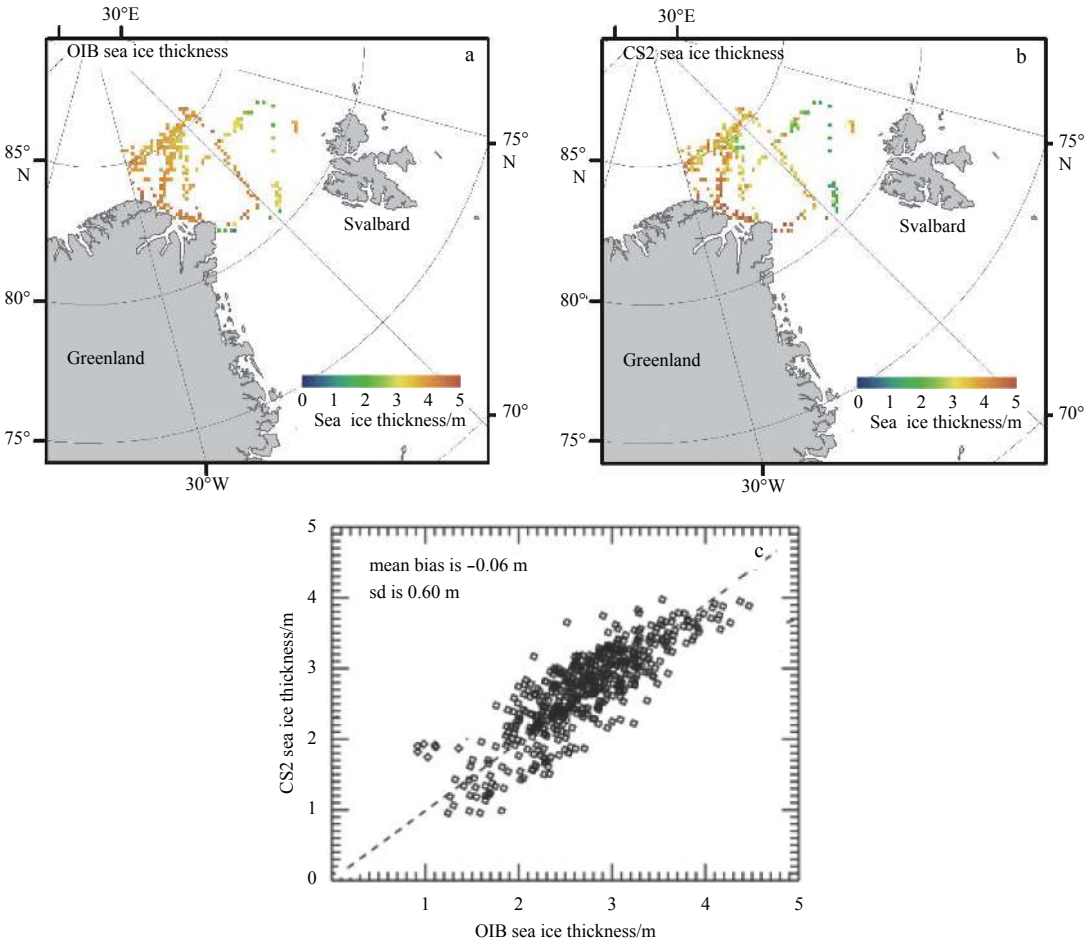

Fig. 2. Footprints of OIB measurements (a) and the corresponding locations and CS2 observations (b) around the FS area for the period of March–April over 2011–2015. Comparative statistics based on the two data sets are illustrated in Fig. 2c. sd refers to the standard deviation of the differences.

product as to the IFREMER). Monthly average ice drift is obtained through averaging all the 3/d IFREMER products of the corresponding month (ftp://ftp.ifremer.fr/ifremer/cersat/products/gridded/psi-drift/data/arctic/). The merged product has a grid size of 62.5 km (Girard-Ardhuin and Ezraty, 2012). Assessments indicated an uncertainty range between 1.0 and 4.0 cm/s by comparing daily IFREMER sea ice drift with buoy observations from the international arctic buoy program (IABP) (Sumata et al., 2014) and global positioning system (GPS) data (Hwang, 2013).

2.2.2 *Sea ice concentration*

Sea ice concentration data (1978 to present, Version 2.0) are obtained from NSIDC (http://nsidc.org/data/NSIDC-0079). These to data are derived from Nimbus-7 SMMR and the defense meteorological satellite program (DMSP) SSM/I observations using Bootstrap algorithm (Comiso, 2000). Monthly mean concentrations are available from NSIDC on a polar stereographic projection with a grid size of 25 km.

2.2.3 *Sea ice thickness*

Satellite altimeter data have been acquired by the SIRAL instrument onboard CS2. These data are available in a repository within the ESA data portal (https://earth.esa.int). The pulse-Doppler-limited footprint of the synthetic aperture radar altimeter is approximately 0.31 km by 1.67 km along- and across-track, and multiple-looks of each point on the surface are used to reduce noise caused by radar speckle (ESA, 2013). For a full description of the CS2 mission, processing and data products, see Wingham et al. (2006).

The sea ice thickness derived from CS2 altimeter data is provided by the Jet Propulsion Laboratory (JPL), a division of the National Aeronautics and Space Administration (NASA). The monthly mean thickness for cold episodes (October through May) over a 5 a period (2011–2015) are available at http://rkwok.jpl.nasa.gov/cryosat/. This gridded data product has a cell size of 25 km×25 km. Evaluations implemented by Kwok and Cunningham (2015) yield average differences between the CS2-derived sea ice thickness and various field measurements, ranging from –0.16 to 0.06 m with standard deviations between 0.29 and 0.87 m and correlations between 0.53 and 0.79. See Kwok and Cunningham (2015) for more details about the evaluations for the JPL's CS2 sea ice thickness.

In this study, we assess the CS2 sea ice thickness in the FS region using ice thickness from NASA's operation IceBridge (OIB) (Fig. 2). The sea ice thickness from the OIB is retrieved from sea ice freeboard (ice plus snow above the sea surface) measured by a lidar instrument, namely an Airborne Topographic Mapper (ATM). The measurements have a nominal 1 m resolution over a swath approximately 200 m wide and are averaged to give a mean sea ice freeboard for 40 m segments of the flight line. Therefore, each data point represents a 40 m by 200 m area. The obtained ice freeboard is then converted to ice thickness, under the assumption of hydrostatic equilibrium. The OIB missions provide long transects (sometimes more than 3 000 km) that survey the ice cover of the western Arctic between Alaska and Greenland. The OIB data have been obtained from the NSIDC (http://nsidc.org/data/idcsi4). The uncertainties of the OIB ice thickness are variable according to the determination of a sea surface height and the quality of snow depth estimates (Kurtz et al., 2013). In our experiment, data near the FS flux gate from OIB campaigns that took place during March and/or April over the period of 2011 to 2015 are exploited (Fig. 2).

We first average monthly OIB sea ice thickness estimates on a grid using a drop-in-the-bucket method. In other words, gridded OIB data in common with CS2 grid are obtained. The monthly CS2 data from March and April are then compared with the corresponding gridded OIB thickness fields of the same month. Figure 2a shows the locations of the OIB data used to evaluate the corresponding CS2 sea ice thickness data as shown in Fig. 2b. Figure 2c illustrates the comparative results and shows a larger CS2-derived sea ice thickness compared with the OIB sea ice thickness in the FS region, with an average bias of 0.06 (±0.60) m and a correlation of 0.75 between the two data. The number after a "±" refers as to the standard deviation (SD) of the differences. The larger difference mainly appears over the north of Svalbard Island while north of Greenland the difference is small. The greater bias is largely explained by the thickness category between 0 and 2 m as shown in the east of Svalbard, while smaller bias is identified among the thicker sea ice as shown in the North Greenland (Figs 2a and b).

In this study, a comparison of our recent CS2-derived volume flux (2011/2012–2014/2015) with previous results is conducted. For consistency, we recalculate the FS volume flux based on two earlier sea ice thickness record for the period of 1991/1992–1998/1999 when moored ULS observation is available and for the period of 2003/2004–2007/2008 when ICESat-derived sea ice thickness is achieved.

2.2.4 *ULS-based sea ice volume flux*

A record of sea ice volume flux (1991–2013) provided by Spreen G. of the University of Bremen (personal communication) is compared with our estimates (Spreen et al., 2016). It is calculated using the NSIDC sea ice drift in combination with sea ice thickness profiles inferred from three or four ULS measurements deployed around 79°N between 2°W and 8°W (Spreen et al., 2006; Hansen et al., 2013, 2014, 2015). For the period from January 2011 to August 2013, the uncertainty of 259 km^3 in their WAVF corresponds to 29% of its mean estimate (889 km^3).

3 Results

3.1 *Monthly sea ice volume flux*

Figure 3 shows the monthly sea ice volume flux during the winter (October–April) for the period of 2011–2015, which is calculated from different sea ice drift data products (IFREMER in red and NSIDC in blue as shown in Fig. 3). The correlation between the monthly area fluxes from the NSIDC and the IFREMER is high (R=0.85). For the NSIDC-based sea ice area flux, there are average bias of (–18×10^3±15) km^2 in monthly export in comparison with those derived from the IFREMER sea ice drift data (Table 1). The numbers after "±"refer as to the standard deviation of the difference. The correlation between the volume flux estimates based on the NSIDC and IFREMER sea ice drifts is 0.54. The mean monthly difference between the NSIDC- and IFREMER-based sea ice volume flux is (–62±84) km^3 (Table 1). Therefore, the NSIDC-based sea ice area fluxes relatively underestimate the results compared with those from the IFREMER data.

The WAVF through FS over the period of 2011/2012–2014/2015, on average, amounts to 504×10^3 and 378×10^3 km^2 for the sea ice area fluxes estimated from the IFREMER and NSIDC sea ice drifts, respectively (Table 1). Following Eq. (3), an average uncertainty of 6.4×10^3 km^2 per month (19.2 km^3 per month) in the monthly sea ice area flux (sea ice volume flux) based on the IFREMER sea ice drift is determined (Table 1). This quantity amounts to 8.8% of the average monthly sea ice area flux (72×10^3 km^2 per month), and 9.0% of the mean monthly sea ice volume flux (209

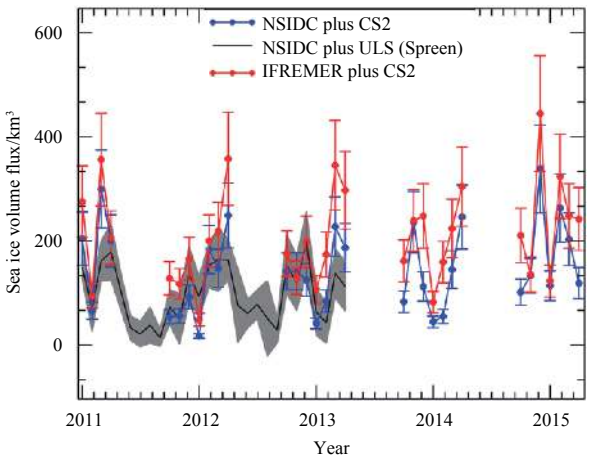

Fig. 3. Monthly estimates of sea ice volume flux and corresponding uncertainty based on Cyrosat-2 sea ice thickness and IFREMER (red) and NSIDC (blue) sea ice drift data. A short-term (January 2011 to August 2013) estimate of sea ice volume flux (black), with it uncertainty range (gray shade), based on NSIDC sea ice drift and ULS sea ice thickness, provided by Spreen G is added in the plot.

km³ per month). The average monthly uncertainty, approximately 7.2×10^3 km² per month (21 km³ per month) in the sea ice area flux (sea ice volume flux) based on the NSIDC sea ice drift corresponds to 13.3% (14.3%) of the average monthly sea ice area flux (volume flux) estimate of 54×10^3 km² per month (147 km³ per month).

In terms of the F_{WAVF} following Eq. (4), the estimates amount to 1 463 km³ (IFREMER) and 1 029 km³ (NSIDC) (Table 1). Following Eq. (5), the average uncertainty of the F_{WCF} estimated from the NSIDC (IFREMER) sea ice drift data is computed as 55.5 km³ (50.8 km³) (Table 1). These quantities correspond to 5.4% (or 3.5%) of the mean WAVF based on the NSIDC (or IFREMER) sea ice drift product.

The sea ice volume flux is further compared to results provided by Spreen G. in the University of Bremen (UB) (see the black line with the gray shade in Fig. 3). The UB-sea ice volume flux is calculated from the NSIDC sea ice drift and ULS measurements of sea ice thickness. Time series of the UB's sea ice volume flux is overlapped with our winter sea ice volume flux over the period of January 2011 to August 2013. The comparative results reveals an average bias of (5.7±45.9) km³ per month between our and UB's monthly sea ice outflow estimates. For the winter months, the variations of our estimates are generally within the standard deviations of the UB estimates (shaded area in Fig. 3) and the temporal variability of the two estimates is correlated well (R=0.68). Since the two sea ice volume flux estimates are both derived from the NSIDC sea ice drift data, the deviations between the two sea ice volume flux estimates are largely controlled by the differences between the sea ice thickness fields employed (CS2 vs ULS).

The mean monthly FS sea ice outflow (seasonal cycle) from the IFREMER and NSIDC sea ice drift products is presented in Fig. 4. A relatively larger sea ice area/volume flux is identified in the former compared with latter estimates (Fig. 4), with a mean difference of approximately 12×10^3 km² per month (sea ice area flux) and 20 km³ per month (volume flux). However, the two estimates generally agree with each other within one standard deviation (Fig. 4), and the temporal variability between the two FS sea ice outflow estimates is in good agreement.

3.2 *Winter sea ice volume flux for different periods*

To understand the changes of the FS sea ice volume exports, the F_{WAVF} based on NSIDC and IFREMER drifts (Fig. 5) are obtained for three periods when sea ice thickness in FS is available,

Table 1. Mean estimate and uncertainty of sea ice area and volume fluxes based on the IFREMER and NSIDC drifts over the period of 2011–2015

		Mean monthly outflow	Uncertainty for mean monthly outflow	Mean winter outflow (Oct. – Apr.)	Uncertainty for mean winter outflow
Area flux/km²	IFREMER	72×10^3	6.4×10^3	504×10^3	16.9×10^3
	NSIDC	54×10^3	7.2×10^3	378×10^3	19.0×10^3
Volume flux/km³	IFREMER	209	19.2	1 463	50.8
	NSIDC	147	21.0	1 029	55.5

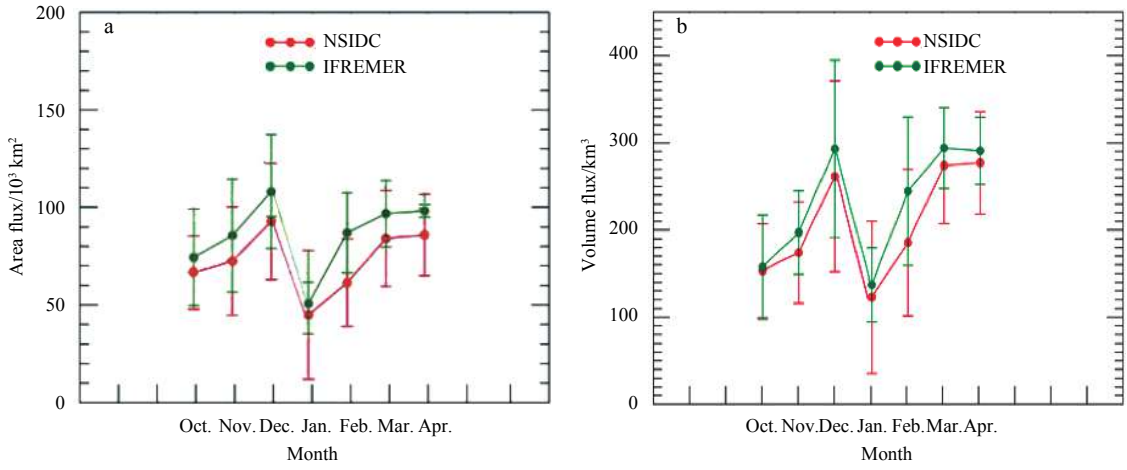

Fig. 4. Mean monthly sea ice area flux (a) and volume flux (b) through the FS for the period of 2011–2015.

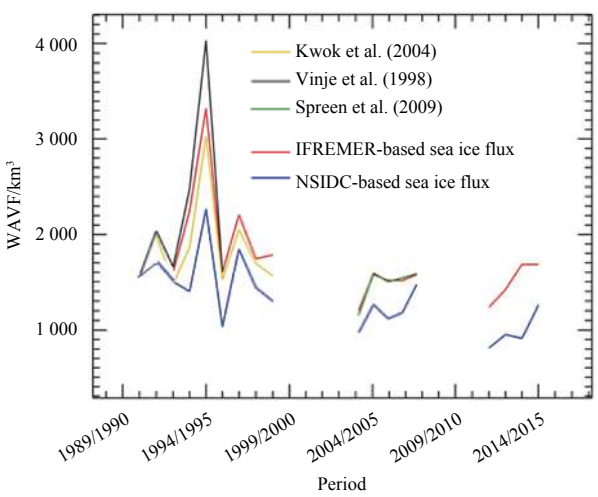

Fig. 5. F_{WAVF} estimates based on different drift products and comparisons with those from previous studies. The estimates based on IFREMER (red) and NSIDC (blue) sea ice drift products and CS2 sea ice thickness data are represented by red and blue color, respectively. The yellow, black and green lines denote the sea ice volume flux estimates reported in Kwok et al. (2004), Vinje et al. (1998), and Spreen et al. (2009).

including P1 (1991/1992–1998/1999), P2 (2003/2004–2007/2008), and P3 (2011/2012–2014/2015). The selection of the three periods is based on the availability of the sea ice thickness record. The two earlier periods represent the era when well-assessed sea ice volume flus results were published and could be accessed. A glimpse of the rapid decline in the winter FS sea ice volume exports is seen in Fig. 5 and quantitative details are summarized in Table 2. An earlier estimate of the FS sea ice volume flux for the 1990s, with an average winter (October to May) sea ice export of 1 745 km³, is presented in Kwok and Rothrock (1999) and (Kwok et al., 2004). Estimates in Spreen et al. (2009) are computed with the IFREMER (AMSR-E merged) sea ice drifts and the ICESat-derived sea ice thickness. Our mean WAVF from October to April for the period (2011/2012–2014/2015) amounts to 1 463 km³ (IFREMER) and 1 029 km³ (NSIDC), respectively. The IFREMER-based sea ice volume flux is comparable to that provided in Spreen et al. (2009) of 1 564 km³ for the period of P2.

Recall that early studies utilized different input data to derive the sea ice export (Vinje et al., 1998; Kwok et al., 2004; Spreen et al., 2009), a straightforward comparison of our volume flux estimates with previous results may bear some uncertainties due to the potential issue of data incompatibility. In our calculations, the ULS (Vinje et al., 1998), ICESat (Spreen et al., 2009) and CS2 sea ice thickness (Kwok and Cunningham, 2015) is used for the P1, P2 and P3 period, respectively. The systematic bias of the sea ice thickness between the CS2 and ULS observations of 0.07 m (Kwok and Cunningham, 2015), between ICESat and ULS of –0.14 m (Kwok et al. 2009), and between ICESat and CS2 of –0.21 m (Laxon et al., 2013; Kwok and Cunningham, 2015), has been removed before the calculation of our sea ice volume flux.

Our estimates for winter export, based on the NSIDC and IFREMER sea ice product, show a similar decline over periods from P1 to P3. On average, NSIDC-based winter flux (October–May) show a decline of 571 km³ (or 33.0% of mean export in P1) between P1 and P2 and an relatively small reduction of 39 km³ (or 3.4% of mean export for P2) from P2 to P3. The winter (October–April) sea ice volume outflow derived from the IFREMER data is also suggestive of a dramatic decline between P1 and P2 (561 km³ or 26.8% of mean export in P1) and a relatively small decrease between P2 and P3 (78 km³ or 5.1% of mean flux in P2). For available summer FS volume exports (June–September), NSIDC-based estimates show a slight change of –18 km³ between P1 and P3 (not shown).

For the overlapped period, our estimates derived from the IFREMER sea ice drifts is less than those of Vinje et al. (1998) (black line in Fig. 5), but larger than those of Kwok et al. (2004) (yellow line in Fig. 5). Indeed, several studies have also demonstrated the fact that the NSIDC sea ice drift is slower than most currently available sea ice drift products (Sumata et al., 2014, 2015). Based on our results, it is further verified that the NSIDC-based sea ice export is relatively slower than that from the IFREMER sea icedrifts. More facts about a slower NSIDC sea ice drift is discussed in Section 4.1. On the other hand, Spreen et al. (2009) utilized the IFREMER product from AMSR-E for the FS sea ice export over the P2 period (green line in Fig. 5), which is closely consistent with the estimates based on the IFREMER ASCAT-SSM/I merged product for the same period (red lines as shown in Fig. 5), cross-validating our calculations and giving us confidence in the following analysis.

4 Discussion

4.1 *Understanding the differences of IFREMER and NSIDC sea ice drifts*

A cross-gate sea ice speed difference between the IFREMER and the NSIDC sea ice drift data in the FS region is shown in Fig. 6. Figure 6a illustrates the cross-strait sea ice speed difference in the winter months over the period of 2011–2015. It points to the dominance of larger IFREMER sea ice drift speeds as indicated by the warm colors. Indeed, about 73% of the 224 winter months for the 5 a (2011–2015) had faster IFREMER sea ice drift speeds than the NISDC sea ice drifts (Fig. 6a). The overall average difference in sea ice drift speeds between the two sea ice drift data (i.e., IFREMER minus NSIDC) is (3.1±3.0) km/d with a correlation of 0.74 (Fig. 6b). Therefore, the relatively higher IFREMER sea ice drift speeds, compared with those of the NSIDC, explains the lar-

Table 2. WAVF estimates based on NSIDC and IFREMER sea ice drifts for different periods (P1: 1991/1992–1998/1999, P2: 2003/2004–2007/2008, and P3: 2011/2012–2014/2015) and the changes between different periods

	NSIDC	IFREMER
	WAVF (Oct. –May)/km³	WAVF (Oct. –Apr.)/km³
P1 (1991/1992–1998/1999)	1 731	2 089
P2 (2003/2004–2007/2008)	1 160	1 528
P3 (2011/2012–2014/2015)	1 121	1 450
P2 minus P1	–571	–561
P3 minus P2	–39	–78
P3 minus P1	–610	–639

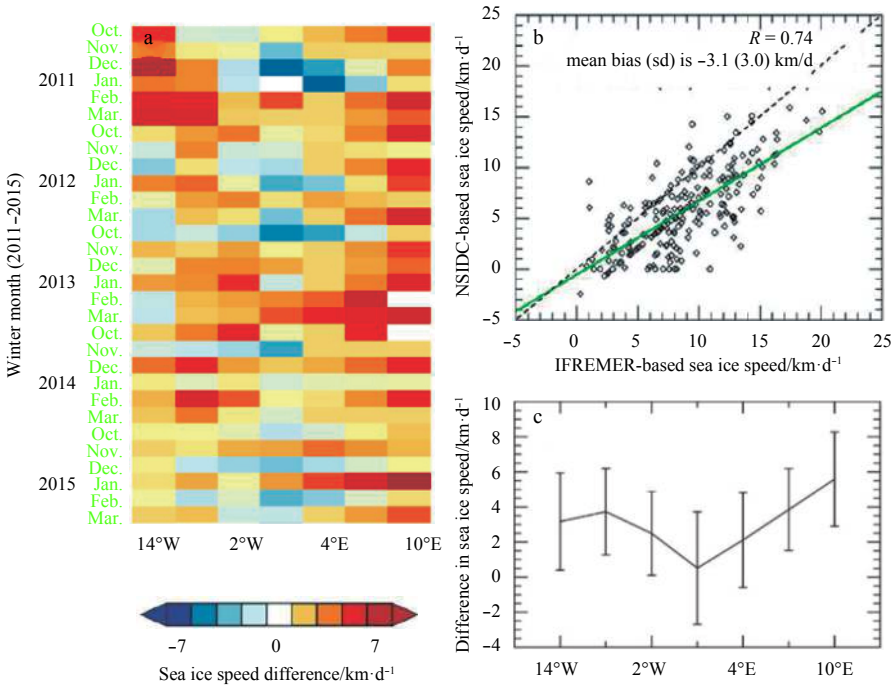

Fig. 6. FS cross-gate (14°W–10°E) sea ice drift speed differences between IFREMER and NSIDC sea ice drifts. The comparisons are illustrated as monthly difference map (a) and scatter plot (b). The black dash line in Fig. 6b is the one-to-one line and the green bold line denote the linearly fitted line between the two data. The five-year mean cross-gate difference is marked in Fig. 6c.

ger sea ice volume flux estimates as mentioned in the above analysis. Geographically, the grid in the central zone of the FS shows the lowest bias while grids towards the west and east coasts have increasingly larger IFREMER sea ice speeds compared with the NSIDC data (Fig. 6c).

Sumata et al. (2014) conducted a recent study to assess the uncertainty estimates for all publicly available satellite-derived sea ice drift products, including ocean and sea ice satellite application facility (OSISAF), NSIDC, IFREMER, and IABP observations from Kimura et al. (2013). They conclude that sea ice drift bias and uncertainty are related to (1) satellite data input, (2) sea ice-tracking algorithm, (3) interpolation techniques, and (4) spatial and temporal scales evaluated. Sumata et al. (2014) find that the NSIDC is relatively small compared with above sea ice drift products, and Sumata et al. (2015) confirms a slower NSIDC sea ice drift than the above-mentioned satellite-derived sea ice drift products, when assessed with sea ice drift retrieved from high-resolution SAR imagery. Furthermore, Studies of Szanyi et al. (2016) document a large systematic error (bias) in the NSIDC sea ice drift product, and identify one source for this high random error and bias is associated with the direct assimilation of small-scale buoy velocity into the large-scale sea ice drift velocity field inferred from satellites. In addition, Bi et al. (2016b) reported a smaller NSIDC-based sea ice volume flux through the FS compared with those provided by Kwok (2009).

4.2 *Attributions to the WAVF changes between different periods*

In this part, long-term WAVF changes are attributed to the changes in sea ice motion, the sea ice concentration and the sea ice thickness. As revealed in Fig. 7, a decline has been identified in the mean WAVF estimates based on the IFREMER and NSIDC sea ice drift data over the three study periods (P1, P2 and P3). Meanwhile, the satellite-derived results suggest a significant decline in the FS sea ice drift took place over the three periods. Generally, the temporal behavior of sea ice motion determines the sea ice volume changes (Fig. 7a vs Fig. 7b). The similar declined

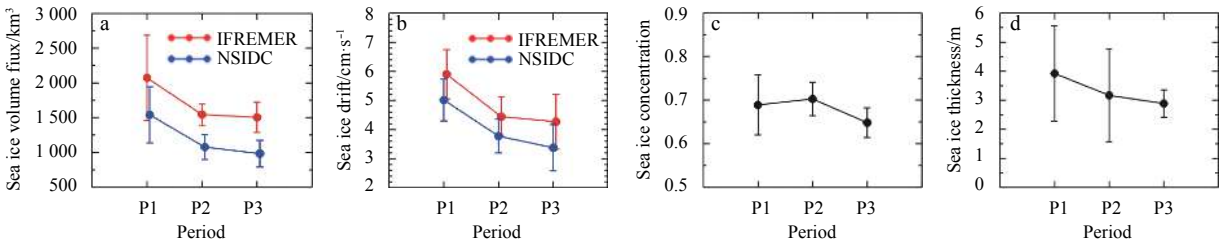

Fig. 7. Changes for WAVF over different periods and relevant parameters to influence on the sea ice flux changes, including sea ice motion (b), sea ice concentration (c), and sea ice thickness (d). The mean and uncertainty (error bar) estimates are calculated over different periods: P1 (1991/1992–1994/1995), P2 (2003/2004–2007/2008), and P3 (2010/2011–2014/2015). Different sources of estimates of the sea ice volume flux and sea ice motion, based on the IFREMER (red) and NSIDC (blue) drift data, are given in the plots (a) and (b).

magnitude of sea ice motion is noted in the results based on the two sea ice drift products. On the basis of these satellite-derived results, Fig. 7b indicates a remarkable decline (by about –1.5 cm/s) in mean sea ice motion from P1 to P2 and relatively small decline (by less than 0.5 cm/s) between P2 and P3.

The decline in sea ice motion further enhanced by a continuous decline in the satellite-derived sea ice thickness field has been encountered the in FS region, from approximately 4.0 to 2.6 m, on average (Fig. 7d). The similar trend of sea ice thinning in the FS region has also been affirmed in recent studies (Hansen et al., 2013, 2014, 2015) and also over the Arctic Ocean (Kwok and Rothrock, 2009). The sea ice concentration seems to contribute to a minor percentage with respect to the changes in the sea ice volume flux. The mean sea ice concentration in the first two periods remains insignificantly changed, while a relatively noticeable decrease is found in P3, approximately by 0.05% or 7% compared with the mean sea ice concentration (0.7) in P2. Therefore, the satellite-derived sea ice concentration decrease accounts for the least contribution to the sea ice volume flux changes.

5 Concluding remarks

Motivated by the current availability of the CS2 sea ice thickness data, the sea ice volume flux through the FS was estimated for the winter months during the recent 5 a period (2011–2015). Over this period, the average winter (October–April) accumulative sea ice volume flux, based on the sea ice drift data derived from passive-microwave measurements provided by the NSIDC and the IFREMER, amounted to 1 029 and 1 463 km^3, respectively. Meanwhile, differences in the sea ice area and volume flux estimates between the IFREMER and the NSIDC derived products were identified. On average, the IFREMER product indicates a faster sea ice drift relative to the NSIDC sea ice drift. As a result, the mean monthly sea ice area flux (volume flux) derived from the IFREMER data was 18×10^3 km^2 per month (62 km^3 per month) greater than those derived from the NSIDC data. With respect to the changes, the sea ice volume flux underwent a large decline between P1 and P2, but remains relatively stable between P2 and P3. Among the variables associated with the volume flux, the sea ice motion controls the behavior of sea ice volume flux, the sea ice thickness further enhances the decline over periods, while the sea ice concentration contributes to a minor impacts on the sea ice volume flux changes.

As indicated by the FS sea ice volume flux reduction of –639 km^3 (IFREMER) and –610 km^3 (NSIDC), a remarkable salt perturbation over the downstream of the Fram Strait in the North Atlantic seas is expected. As a result, convective exchange processes in the North Atlantic seas that occur due to the advection and melt sea ice could be altered and the formation of deep water could be influenced (Ionita et al., 2016). Some evidence has demonstrated that a substantial freshening of the northern North Atlantic during the period of 1965–1995 was partially linked to the increased sea ice export and melt during that period (Peterson et al., 2006). In the future work, both field and satellite observations, in concert with sophisticated modelling work, are encouraged to investigate the far-reaching oceanographic and atmospheric implications of changes in the sea ice outflow through the FS.

Acknowledgements

The authors thank the following organizations for providing the data used in this study: the NSIDC (ice concentration, motion), the IFREMER (sea ice drift), and the JPL (Cryosat-2 thickness).

References

Bi Haibo, Huang Haijun, Fu Min, et al. 2016a. Estimating sea-ice volume flux out of the Laptev Sea using multiple satellite observations. Polar Research, 35(1): 24875

Bi Haibo, Sun Ke, Zhou Xuan, et al. 2016b. Arctic sea ice area export through the Fram Strait estimated from satellite-based data: 1988-2012. IEEE Journal of Selected Topics in Applied Earth Observations and Remote Sensing, 9(7): 3144–3157

Comiso J C. 2000. Bootstrap Sea Ice Concentrations from Nimbus-7 SMMR and DMSP SSM/I-SSMIS, Version 2. Boulder, Colorado USA: NASA National Snow and Ice Data Center Distributed Active Archive Center

Comiso J C. 2012. Large decadal decline of the Arctic multiyear ice cover. Journal of Climate, 25(4): 1176–1193

ESA. 2013. CryoSat Product Handbook, April 2013. London, UK: ESRIN-ESA and Mullard Space Science Laboratory University College London

Giles K A, Laxon S W, Ridout A L. 2008. Circumpolar thinning of Arctic sea ice following the 2007 record ice extent minimum. Geophysical Research Letters, 35(22): L22502

Girard-Ardhuin F, Ezraty R. 2012. Enhanced Arctic sea ice drift estimation merging radiometer and scatterometer data. IEEE Transactions on Geoscience and Remote Sensing, 50(7): 2639–2648

Hansen E, Ekeberg O C, Gerland S, et al. 2014. Variability in categories of Arctic sea ice in Fram Strait. Journal of Geophysical Research: Oceans, 119(10): 7175–7189

Hansen E, Gerland S, Granskog M A, et al. 2013. Thinning of Arctic sea ice observed in Fram Strait: 1990-2011. Journal of Geophysical Research: Oceans, 118(10): 5202–5221

Hansen E, Gerland S, Høyland K V, et al. 2015. Time variability in the annual cycle of sea ice thickness in the Transpolar Drift. Journal of Geophysical Research: Oceans, 120(12): 8135–8150

Hwang B. 2013. Inter-comparison of satellite sea ice motion with drifting buoy data. International Journal of Remote Sensing, 34(24): 8741–8763

Ionita M, Scholz P, Lohmann G, et al. 2016. Linkages between atmospheric blocking, sea ice export through Fram Strait and the Atlantic meridional overturning circulation. Scientific Reports, 6: 32881

Kimura N, Nishimura A, Tanaka Y, et al. 2013. Influence of winter sea-ice motion on summer ice cover in the Arctic. Polar Research, 32(1): 20193

Koenigk T, Mikolajewicz U, Haak H, et al. 2006. Variability of Fram Strait sea ice export: causes, impacts and feedbacks in a coupled climate model. Climate Dynamics, 26(1): 17–34

Krumpen T, Gerdes R, Haas C, et al. 2016. Recent summer sea ice thickness surveys in Fram Strait and associated ice volume fluxes. The Cryosphere, 10(2): 523–534

Krumpen T, Janout M, Hodges K I, et al. 2013. Variability and trends in Laptev Sea ice outflow between 1992–2011. The Cryosphere, 7(1): 349–363

Kurtz N T, Farrell S L, Studinger M, et al. 2013. Sea ice thickness, freeboard, and snow depth products from Operation IceBridge airborne data. The Cyrosphere, 7(4): 1035–1056

Kwok R. 2009. Outflow of Arctic Ocean sea ice into the Greenland and Barents Seas: 1979–2007. Journal of Climate, 22(9): 2438–2457

Kwok R, Cunningham G F. 2015. Variability of Arctic sea ice thickness and volume from CryoSat-2. Philosophical Transactions of the Royal Society A: Mathematical, Physical and Engineering Sciences, 373(2045): 20140157

Kwok R, Cunningham G F, Pang S S. 2004. Fram Strait sea ice outflow. Journal of Geophysical Research: Oceans, 109(C1): C01009

Kwok R, Cunningham G F, Wensnahan M, et al. 2009. Thinning and volume loss of the Arctic Ocean sea ice cover: 2003–2008. Journal of Geophysical Research: Oceans, 114(C7): C07005

Kwok R, Maslowski W, Laxon S W. 2005. On large outflows of Arctic sea ice into the Barents Sea. Geophysical Research Letters, 32(22): L22503

Kwok R, Rothrock D A. 1999. Variability of Fram Strait ice flux and North Atlantic oscillation. Journal of Geophysical Research: Oceans, 104(C3): 5177–5189

Kwok R, Rothrock D A. 2009. Decline in Arctic sea ice thickness from submarine and ICESat records: 1958–2008. Geophysical Research Letters, 36(15): L15501

Laxon S W, Giles K A, Ridout A L, et al. 2013. CryoSatA L nnual variability of sea ice thickness in the A. Geophysical Research Letters, 40(4): 732–737

Laxon S, Peacock N, Smith D. 2003. High interannual variability of sea ice thickness in the Arctic region. Nature, 425(6961): 947–950

Lei R B, Heil P, Wang J, et al. 2016a. Characterization of sea-ice kinematic in the Arctic outflow region using buoy data. Polar Research, 35(1): 22658

Lei R B, TianR58.sear, Leppäranta M, et al. 2016b. Changes in summer sea ice, albedo, and portioning of surface solar radiation in the Pacific sector of Arctic Ocean during 1982–2009. Journal of Geophysical Research: Oceans, 121(8): 5470–5486

Meier W N. 2005. Comparison of passive microwave ice concentration algorithm retrievals with AVHRR imagery in arctic peripheral seas. IEEE Transactions on Geoscience & Remote Sensing, 43(6): 1324–1337

Peterson B J, McClelland J, Curry R, et al. 2006. Trajectory shifts in the Arctic and subarctic freshwater cycle. Science, 313(5790): 1061–1066

Serreze M C, Holland M M, Stroeve J. 2007. Perspectives on the Arctic's shrinking sea-ice cover. Science, 315(5818): 1533–1536

Smedsrud L H, Halvorsen M H, Stroeve J C, et al. 2017. Fram Strait sea ice export variability and September Arctic sea ice extent over the last 80 years. The Cryosphere, 11(1): 65–79

Spreen G, Kern S, Stammer D, et al. 2006. Satellite-based estimates of sea-ice volume flux through Fram Strait. Annals of Glaciology, 44(1): 321–328

Spreen G, Kern S, Stammer D, et al. 2009. Fram Strait sea ice volume export estimated between 2003 and 2008 from satellite data. Geophysical Research Letters, 36(19): L19502

Spreen G, Kwok R, Hansen E, et al. 2016. Arctic sea ice volume export through Fram Strait from combined satellite and upward looking sonar (ULS). In: ESA Living Planet Symposium 2016. Prague, Czech Republic

Steele M, Ermold W. 2015. Loitering of the retreating sea ice edge in the Arctic Seas. Journal of Geophysical Research: Oceans, 120(12): 7699–7721

Stroeve J, Notz D. 2015. Insights on past and future sea-ice evolution from combining observations and models. Global and Planetary Change, 135: 119–132

Sumata H, Gerdes R, Kauker F, et al. 2015. Empirical error functions for monthly mean Arctic sea-ice drift. Journal of Geophysical Research: Oceans, 120(11): 7450–7475

Sumata H, Lavergne T, Girard - Ardhuin F, et al. 2014. An intercomparison of Arctic ice drift products to deduce uncertainty estimates. Journal of Geophysical Research: Oceans, 119(8): 4887–4921

Szanyi S, Lukovich J V, Barber D G, et al. 2016. Persistent artifacts in the NSIDC ice motion data set and their implications for analysis. Geophysical Research Letters, 43(20): 10800–10807

Vinje T. 2001. Fram Strait ice fluxes and atmospheric circulation: 1950–2000. Journal of Climate, 14(16): 3508–3517

Vinje T, Nordlund N, Kvambekk Å. 1998. Monitoring ice thickness in Fram Strait. Journal of Geophysical Research: Oceans, 103(C5): 10437–10449

Wingham D J, Francis C R, Baker S, et al. 2006. CryoSat: a mission to determine the fluctuations in earth's land and marine ice fields. Advances in Space Research, 37(4): 841–871

Zhang J L, Rothrock D, Steele M. 2000. Recent changes in Arctic sea ice: the interplay between ice dynamics and thermodynamics. Journal of Climate, 13(17): 3099–3114